Hindawi
Mathematical Problems in Engineering
Volume 2022, Article ID 7975101, 16 pages
https://doi.org/10.1155/2022/7975101

Research Article

Comparative Evaluation of the Optimal Auxiliary Function Method and Numerical Method to Explore the Heat Transfer between Two Parallel Porous Plates of Steady Nanofluids with Brownian and Thermophoretic Influences

Hakeem Ullah,[1] **Rafaqat Ali Khan**,[1] **Mehreen Fiza**,[1] **Saeed Islam**,[1] **and Seham M. Al-Mekhlafi**[2]

[1]*Department of Mathematics, Abdul Wali Khan University, Mardan 23200, KP, Pakistan*
[2]*Department of Mathematics, Sanna University, Sana'a, Yemen*

Correspondence should be addressed to Mehreen Fiza; drmehreenfiza@gmail.com and Seham M. Al-Mekhlafi; smdk100@gmail.com

Received 19 February 2022; Revised 20 April 2022; Accepted 17 May 2022; Published 1 July 2022

Academic Editor: Arshad Riaz

In this study, we used the newly established optimal approach, namely, optimal auxilary function method (OAFM) along with the Adams numerical solver technique in order to investigate the heat transfer between two permeable parallel plates of steady nanofluids (HTBTP-SNFs) through Brownian and thermophoretic consequences. The new scheme model (HTBTP-SNFs) in terms of partial differential equations (PDEs) is changed to nonlinear ordinary differential equations (ODEs) by utilizing similarity transformations. The OAFM and Adams numerical methods are used to solve the resulting ODEs with boundary conditions. The OAFM along with convergence and Adams numerical method are studied in detail. The influences of the physical parameters of HTBTP-SNFs model for instance porosity parameter (m), parameter of magnetic (M), parameter of Brownian (Nb), viscosity parameter (R), Schmidt number (Sc), thermophores parameter (Nt), and Prandlt number (Pr) are discussed with the help of tabular data and graphs. The reliability and effectiveness of the technique are achieved by equating the results available in the literature.

1. Introduction

Energy is incredibly essential in today's world. Nanofluids show a significant title part in the industrial sector by enhancing heat transfer processes. Despite their wide variety of applications, heat transfers of nanofluids have become more essential in engineering and industrial innovations. Nanofluids are made up of nanoparticle-sized specks in fluid-termed nanoparticles. Nanofluids are particularly beneficial in managing cooling difficulties in many thermal structures. Maximum thermal conductivity can be beneficial in coolants, lubricants, automatic fluid diffusion, and engine oils. On the other hand, solid nanoparticles with minimal thermal conductivity, can improve the thermal conductivity of fluids [1]. Choi et al. [2, 3], the pioneers of nanofluid research, computed thermal conductivity and demonstrated thermal conductivity enhancement. In a base fluid, Choi and Eastman scrutinized the suspension of nanoparticles for the first time [4]. Shehzad et al. [5] studied the influence of heat transfer of nanofluid within a wavy channel by applying the Buongiorno paradigm. Xuan and Li [6] detected the proficiency of the heat transfer flow in the nanofluid. A great deal of study has on several fluid models [7–12]. Carbides, metals, carbon nanotubes, and oxides are commonly used as nanoparticles. The significance of nanofluids for convective heat transfer usages in determining their appropriateness has been discovered to be highly essential [13, 14]. Nanofluids are colloidal deferments of base fluid nanoparticles that have been manufactured [15, 16]. Oil, ethylene glycol, and water are the most common base fluids. In most research, nanofluid has assumed a normal pure fluid. In renewable energy system and in industrial thermal management, they discovered that utilizing a revolving magnetic disk improves the rate of heat transfer. The investigators looked at several models and physical effects for heat transfer and nanofluid flow improvement [17–27]. Nanofluids also have valuable audial characteristics, in ultrasonic environments demonstrating more shear wave reconversion of an occurrence compression wave; the impact gets further dramatic as concentration rises [28]. Nanofluids have a potential function in the manufacture of airplanes, micromachineries, microdevices, vehicles, and other items, according to the current technology.

In a variety of heat transfer applications, nanofluids have numerous properties that make them potentially useful, such as machining, pharmaceutical procedures, fuel cells, vehicle cooling/thermal control, domestic refrigerators, hybrid-powered engines, chillers, microelectronics, lowering boiler flue gas temperature, and heat exchangers [29]. Zubaidi et al. [30–31] has a great contribution regarding heat transfer applications of nanofluids. Jou and Tzeng [32] quantitatively investigated the vital convection enhancement of a two-dimensional nanofluid. The rise in the average coefficient of heat transmission is evident when the parameter of buoyancy and the nanofluid volume percentage are increased. Rashidi and Pour [33] simulate the fluid moving above the permeable rotating disc when using the second thermodynamic law to an electrically behaving incompressible nanofluid.

There are numerous applications of the steady nanofluids and many researchers perform their great work in this regard. Rashidi et al. [34] discussed the entropy generation in steady magneto hydro dynamics flow owing to a rotating permeable disk in a nanofluid. Veera Krishna [35] inspected the application of steady nanofluid on steady magneto hydrodynamics flow of copper and alumina nanofluids as heat transport past a stretching permeable surface; similarly, Lin and Ghaffari [36] discussed the heat and mass transfer above the surface of a stretching wedge in a steady flow of sutter by nanofluid. The literature study reveals that a great deal of significance has pursued in the case of flows in permeable channel. In fluid-saturated permeable channels, the importance of convective flow has been largely motivated by its function in numerous natural and developed challenges in latest studies of concern. Fetecau et al. [37] examined analytical solutions through a porous plate channel relating to unsteady motions of Maxwell fluids for two mixed initial boundary value problems. Zeeshan et al. [38] scrutinized nanofluid of electroosmotic-modulated bioflow induced by complex traveling wave with zeta potential and heat source via a rectangular peristaltic pump. Abel et al. [39] may see the 2nd grade fluid heat transfer with a nonuniform heat sink/source study through a permeable channel from a penetrable stretched sheet in conjunction with the current research. For the analytic approximated solution, Rashidi et al. [40] employed the HAM in a permeable channel for the issue of steady flow on a spinning disk, including two auxiliary parameters. Khalili et al. [41] investigated mass- and time-dependent convective heat transmission in pseudoplastic nanofluids, calculating the nonlinear mechanism beyond a stretched wall using a fourth-order R-K methodology paired with a conventional shooting technique. By making use of two auxiliary parameters, Abolbashari et al. [42] used an analytic approximated solution of the magneto hydrodynamics flow problem of boundary coating continuously flowing through an extending surface, which has been solved using HAM to evaluate the improvement of the solution convergence rate. Similarly, in a 2nd grade fluid to solve the problem of heat transmission, Rashidi et al. [43] used a permeable medium and a modified differential transform method (DTM). Furthermore, to these deterministic techniques, nanosubstances are utilized for the problems of fluid dynamics managed by non-Newtonian fluidics systems [44–47].

Concern with the related investigation many researchers did a tremendous job in the computational analysis of nanofluids. Beside a vertical wavy surface, Iqbal et al. [48] discussed a computational investigation of dissipation influences on the flow of hydro magnetic convective of hybrid nanofluids. Similarly, Ghaffari et al. [49] analyzed entropy generation above a stretchable rotatory permeable disk in a flow of power-law nanofluid. The analytical and numerical approaches investigated have both merits and disadvantages. Numerical techniques necessitated linearization and discretization, which may have an impact on accuracy. Many researchers use analytical methods to solve nonlinear equations, such as the DTM (differential transform method) [50], HPM (homotopy perturbation method) [51, 52], ADM (Adomian decomposition method) [53], VIM (variational iteration method) [54], radial basis function [55], HAM (homotopy analysis method) [56] and artificial parameters method [57, 58]. All of these methods required the assumption of a tiny parameter, such as HPM, or a first guess. Again, poor selection has an impact on accuracy. Currently, Herisanu et al. [59, 60] have proposed an optimum method (OAFM). The small parameter and initial guess assumptions are not necessary in OAFM. We propose the OAFM for the HTBTP-SNF model in this work. The methodology of the Adams numerical technique and OAFM have been formulated in Section 2. The problem formulation and the results assessments have been discussed in Sections 3 and 4, respectively. While the comparison tables of OAFM and Adams numerical method are given in Section 5 (Tables1–3), the conclusion is provided in Section 6.

Table 1: Comparison of the OAFM and Adams numerical method for $f(x)$.

x	OAFM	Numerical solution	Absolute error (AE)
0	0	0	0
0.1	0.0805954451	0.080595445138914	8.9141×10^{-12}
0.2	0.1268821951	0.126882195101887	1.8873×10^{-12}
0.3	0.1453119717	0.145311971751876	1.8761×10^{-12}
0.4	0.1420660044	0.142066004420172	4.2017×10^{-10}
0.5	0.1231630169	0.123163016993000	9.3213×10^{-11}
0.6	0.0945265113	0.094526511335266	3.5266×10^{-11}
0.7	0.0620287942	0.062028794245478	4.5478×10^{-11}
0.8	0.0315236584	0.031523658481825	8.1825×10^{-11}
0.9	0.0088766024	0.008876602424646	2.4646×10^{-11}
1.0	-3.049910×10^{-9}	$-3.0499100129 \times 10^{-9}$	-6.9106×10^{-15}

Table 2: Comparison of the OAFM and Adams numerical method for $g(x)$.

x	OAFM	Numerical solution	Absolute error (AE)
0	1	1	0
0.1	0.890979091	0.89097909180232	8.0232×10^{-10}
0.2	0.783826564	0.78382656476964	7.6964×10^{-11}
0.3	0.678936228	0.67893622838875	3.8875×10^{-11}
0.4	0.5764164678	0.576416467884122	8.4122×10^{-11}
0.5	0.4761733918	0.476173391863718	6.3718×10^{-11}
0.6	0.3779836568	0.377983656802516	2.5161×10^{-11}
0.7	0.2815564324	0.281556432496159	9.6159×10^{-11}
0.8	0.1865863193	0.1865863193618622	1.8622×10^{-11}
0.9	0.0928000588	0.0928000588063435	6.3435×10^{-11}
1.0	-1.025373×10^{-9}	$-1.025373530 \times 10^{-9}$	-7.353×10^{-14}

Table 3: Comparison of the OAFM and Adams numerical method for $h(x)$.

x	OAFM	Numerical solution	Absolute error (AE)
0	1	1	0
0.1	0.9048468313	0.904846831361751	6.1751×10^{-11}
0.2	0.8084909694	0.808490969412694	1.2694×10^{-11}
0.3	0.7109459674	0.710945967436434	3.6434×10^{-11}
0.4	0.6122751974	0.612275197451976	5.1976×10^{-11}
0.5	0.5125576533	0.512557653304655	4.6550×10^{-12}
0.6	0.4118639265	0.411863926563999	6.3999×10^{-11}
0.7	0.3102436548	0.310243654829592	2.9592×10^{-11}
0.8	0.20772288512	0.2077228851230552	3.0552×10^{-12}
0.9	0.10430886568	0.1043088656840427	4.0427×10^{-12}
1.0	$9.4218732 \times 10^{-10}$	$9.4218732684 \times 10^{-10}$	4.4476×10^{-16}

The innovative contributions of computing procedure are as follows:

(i) The numerical and analytical computation have been designed through the technique of Adams numerical solver and optimal auxilary function method (OAFM) for the comparative study to investigate the heat transfer between two permeable parallel plates of steady nanofluids (HTBTP-SNFs) through Brownian and thermophoretic influences.

(ii) The PDEs representing HTBTP-SNFs are converted into a system of ODEs by utilizing appropriate transformation.

(iii) The Mathematica software command "NDSolve" is used to compute the dataset for HTBTP-SNFs for the alternative of parameter of porosity (m), magnetic parameter (M), Brownian parameter (Nb), viscosity parameter (R), Schmidt quantity (Sc), thermophores parameter (Nt), and Prandlt number (Pr).

(iv) The MATLAB software has been used to interpret the solution and the AE analysis plots of HTBTP-SNFs.

(v) The correctness and the validation of the HTBTP-SNFs are examined by both analytical and numerical techniques.

2. Methodology

The methodology in this section includes two parts. Firstly, the formation of data set by the Adams numerical method and secondly, the explanation of fundamental idea of OAFM is illuminated.

2.1. Adams Numerical Method. For the first-order system, the Adams numerical approach is written as

$$\frac{d\zeta}{dx} = f(x,\zeta),$$
$$\chi_{l+1} = \zeta_l + \int_{t_l}^{t_{l+1}} \frac{d\zeta}{dx}dt = \zeta_l + \int_{t_l}^{t_{l+1}} f(\zeta,t)dt, \tag{1}$$

where ζ specifies the first-order output of linear ordinary differential equations (ODEs), x indicates the input value, χ_{l+1}represent the 1^{st} order interpolation iterative structure, and t represents the time interval.

Within the interval $(t_l,\ t_{l+1})$, Adams techniques are grounded on the basis of estimating the integral with a polynomial. Adams approaches are of two kinds, the explicit and the implicit classes. The explicit sort techniques are known as Adams–Bashforth techniques (ABT) while the implicit kinds are called the Adams–Moulton techniques (AMT). The ABT and AMT techniques of the 1^{st} order are the approaches of forward and backward Euler. By applying a linear interpolant, the second-order procedures of these approaches are attained which are very informal. The second-order Adams–Bashforth technique (ABT2) is specified as follows:

$$\chi_{l+1} = \zeta_l + \frac{h}{2}\left(3f\left(\zeta_l, t_l - f\left(\zeta_{l-1}, t_{l-1}\right)\right)\right), \tag{2}$$

where the step interval signify by h. The Adams–Moulton technique of second order (AMT2) is an implicit technique, also inspected to as the principle of trapezoidal specified under

$$\chi_{l+1} = \zeta_l + \frac{h}{2}\left(f\left(\zeta_{l+1}, t_{l+1} + f\left(\zeta_l, t_l\right)\right)\right). \tag{3}$$

2.2. Fundamental Idea of OAFM. For the nonlinear ordinary differential equation of the OAFM,

$$L(g(\xi)) + S(\xi) + N(g(\xi)) = 0, \tag{4}$$

where the operators of linear and nonlinear equations are L and N, S is a source function, and at this phase, the unknown function is $g(\xi)$.

The initial and boundary conditions are

$$B\left(g(\xi), \frac{dg(\xi)}{d\xi}\right) = 0. \tag{5}$$

It is extremely hard to locate out the exact solution of strongly nonlinear equations. The suggested estimated solution is as follows:

$$\widehat{g}(\xi, F_i) = g_0(\xi) + g_1(\xi, F_i), i = 1, 2, \ldots, s. \tag{6}$$

Utilizing equation (6) into equation (4), we obtain

$$L(g_0(\xi)) + L(g_1(\xi, F_i)) + S(\xi) + N(g_0(\xi) + g_1(\xi, F_i)) = 0, \tag{7}$$

where $F_i, i = 1, 2, \ldots, s$ are parameters of control convergence, which are to be concluded.

The initial guess is found out as

$$L(g_0(\xi)) + S(\xi) = 0,$$
$$B\left(g_0(\xi), \frac{g_0(\xi)}{d\xi}\right) = 0. \tag{8}$$

The first approximation is attained as

$$L(g_1(\xi, F_i)) + N(g_0(\xi) + g_1(\xi, F_i)) = 0,$$
$$B\left(g_1(\xi), \frac{g_1(\xi)}{d\xi}\right) = 0. \tag{9}$$

The nonlinear term is given as

$$N(g_0(\xi) + g_1(\xi, F_i)) = N(g_0(\xi)) + \sum_{l=1}^{\infty} u_1^l(t, F_i)N^l(g_0(\xi)). \tag{10}$$

In equation (10), the last term looks tough to solve, thus to depart of this complexity and to the convergence of the solution rapidly, equation (10) can be composed as

$$L(g_1(\xi, F_i)) + D_1((g_0(\xi), F_n)E(N(g_0(\xi)))) + D_2(g_0(\xi), F_m) = 0,$$
$$B\left(g_1(\xi, F_i), \frac{dg_1(\xi, F_i)}{d\xi}\right) = 0, m = 1, 2, \ldots, q, n = q+1, q+2, \ldots s, \tag{11}$$

where the optimal auxiliary functions that depend on $g_0(\xi)$ are D_1 and D_2. While F_m, F_n and $E(N(g_0(\xi)))$are the functions which depend on the expression emerging inside in the nonlinear term of $N(g_0(\xi))$. If $g_0(\xi)$ is polynomial, trigonometric, and exponential, then the optimal auxiliary functions D_1 and D_2 would be the sum of polynomial, trigonometric, and exponential correspondingly. Also, if $N(g_0(\xi)) = 0$, then $g_0(\xi)$ would be the accurate solution of the innovative problem. From the "Galerkin method," "method of least square," "Ritz method," and "collocation method," the optimal auxiliary function method (OAFM) can be achieved.

2.3. Convergence of the Technique. In order to get the convergent solution, we evaluated the optimum constants, which are also recognized as control convergence constants by the "least square method." So, to obtain the series solution, these optimal constants are resubmitted into the original equation:

$$J(F_1, F_2, ..F_s) = \int_I R^2(\xi, F_1, F_2, .., F_s)\mathrm{d}\xi, \tag{12}$$

where I denotes the domain of the equation.

The constants which are unknown can be obtained as

$$\partial_{F_1} J = 0, \partial_{F_2} J = 0, \dots \partial_{F_s} J = 0. \tag{13}$$

3. Problem Formulation

An incompressible laminar steady nanofluid flow has been considered between two horizontal equivalent plates. A coordinate structure in which the both axes x and y are preferred along and normal to the plate. Both fluid and plate are revolving with angular velocity along the y-axis, whereas the bottom plate has stretched by two equal and contrary forces along the x-axis, leaving the location (0, 0) unaltered. As displayed in Figure 1, a uniform and constant magnetic pitch (field) B_0 has provided to the flow in a normal manner. The medium is maintained to be permeable.

The lower plate is permeable and the system is rotating, whereas the flow is subjected to homogeneous magnetic field of density B_0. The governing equations for the suggested fluidic systems are specified as

$$\begin{aligned}
&\frac{\partial u}{\partial x} + \frac{\partial v}{\partial y} = 0\\
&\left(\frac{\partial u}{\partial x}u + \frac{\partial u}{\partial y}v\right)\rho = \left(\frac{\partial^2 u}{\partial x^2} + \frac{\partial^2 u}{\partial y^2}\right)\mu - \frac{\partial p^*}{\partial x} - \sigma B_0^2 u - \frac{\mu}{\eta}u\\
&\rho\left(v\frac{\partial v}{\partial y}\right) = \mu\left(\frac{\partial^2 v}{\partial x^2} + \frac{\partial^2 v}{\partial y^2}\right) - \frac{\partial p^*}{\partial y}\\
&\frac{\partial T}{\partial x}u + \frac{\partial T}{\partial y}v = \alpha\left(\frac{\partial^2 T}{\partial x^2} + \frac{\partial^2 T}{\partial y^2}\right) + \frac{(\rho c_i)_v}{(\rho c_i)_f}\begin{bmatrix} D\left(\dfrac{\partial C}{\partial x} * \dfrac{\partial T}{\partial x} + \dfrac{\partial C}{\partial y} * \dfrac{\partial T}{\partial y}\right) + \\ \left\{\left(\dfrac{\partial T}{\partial x}\right)^2 + \left(\dfrac{D}{T}\right)\left(\dfrac{\partial T}{\partial y}\right)^2\right\}\end{bmatrix}\\
&\frac{\partial C}{\partial y}v + \frac{\partial C}{\partial x}u = \left(\frac{\partial^2 C}{\partial x^2} + \frac{\partial^2 C}{\partial y^2}\right)D_B + \left(\frac{D_T}{T_0}\right)\left\{\frac{\partial^2 T}{\partial x^2} + \frac{\partial^2 T}{\partial y^2}\right\},
\end{aligned} \tag{14}$$

where the velocities of the fluid along axes are u and v, correspondingly. Also, ρ indicates the base fluid density, modified pressure is expressed by p^*, σ denotes the electrical conductivity, μ symbolizes dynamic viscosity, temperature is denoted by T, (μ/η) is porosity parameter, C is concentration, the specific heat of nanofluid is denoted by c_i, and D_B represents the diffusing coefficient of diffusing classes.

$$\begin{aligned}
&u = ax, v = 0, T = T_h, C = C_h, \text{at } y = 0,\\
&u = 0, v = 0, C = C_0, T = T_0, \text{at } y = h.
\end{aligned} \tag{15}$$

Applying the correspondence transformation,

$$\begin{aligned}
&\eta = \frac{y}{h}, u = axf'(\eta), v = -ahf'(\eta),\\
&\phi(\eta) = \frac{C - C_h}{C_0 - C_h}, \theta(\eta) = \frac{T - T_h}{T_0 - T_h}.
\end{aligned} \tag{16}$$

For the dimensionless scheme, together with boundary conditions, the governing equations are stated as

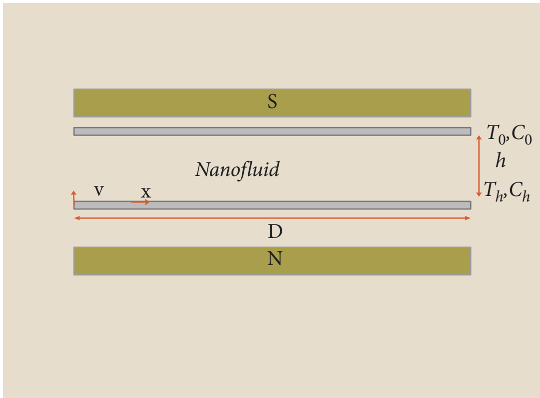

Figure 1: Flow problem geometry.

$$f^{iv} - R\left(f' f'' - f f'''\right) - (M + m) f'' = 0, \tag{17}$$

$$\phi'' + R \bullet Sc f \phi' + \frac{Nt}{Nb}\theta'' = 0, \tag{18}$$

$$R \Pr f\theta' + \theta'' + Nt\theta'^2 + \phi'\theta' Nb = 0. \tag{19}$$

$$\begin{aligned} &f(0) = 0, f'(0) = 1, \theta(0) = 1, \varphi(0) = 1, \\ &f'(1) = 0, f(1) = 0, \theta(1) = 0, \varphi(1) = 0. \end{aligned} \tag{20}$$

The dimensionless quantities are explained as

$$\begin{aligned} R &= \frac{ah^2}{v}, \\ M &= \frac{\sigma B_0^2 h^2}{\rho v}, \\ \Pr &= \frac{\mu}{\rho\alpha}, \\ Sc &= \frac{\mu}{\rho D}, \\ m &= \frac{\mu h^2}{\rho\eta k}, \\ N_b &= \frac{D_B C_h (\rho c)_p}{(\rho c)_f \alpha}, \\ N_t &= \frac{D_T T_h (\rho c)_p}{(\rho c)_f \alpha T_c}, \end{aligned} \tag{21}$$

where the viscosity parameter is R, the magnetic parameter is M, the Prandlt quantity is denoted by Pr, the Schmidt quantity is specified by Sc, m is the porosity parameter, and the Brownian and thermophoretic parameters are specified by Nb and Nt, respectively. Nu represents the Nusselt number and C_f indicates the coefficient of skin friction beside the stretching wall and are specified by

$$\begin{aligned} C_f &= \left(\frac{Rx}{h}\right), \\ C_f &= f''(0), \\ \text{Nu} &= -\theta. \end{aligned} \tag{22}$$

4. Results Assessment

The Adams numerical solver technique has been used for the variants of HTBTP-SNFs model. Numerical and analytical investigation showed the HTBTP-SNFs model has accompanied steady nanofluids between two permeable parallel plates with heat impact, displayed in equations (17)–(20).

Figure 2 shows the mathematical model together with relevant geometry, methodology, and results.

The variation of $M, m, R, \Pr, \text{Sc}, \text{Nb},$ and Nt individually, apiece with three cases of the HTBTP-SNFs model, is tabulated in Table 4.

For velocity profile $f'(\eta)$, temperature distribution $\theta(\eta)$, and concentration distribution $\varphi(\eta)$, the comparative variation of physical parameters of the HTBTP-SNFs model such as magnetic parameter M, parameters of porosity, Brownian motion, viscosity, and thermophoretic are m, Nb, Nt, R, Schmidt number Sc, and Prandlt number Pr through OAFM and Adams numerical method are shown in Figures 3–12, respectively, along with error plots. The consequences of velocity distribution $f'(\eta)$ are given in subfigures 3(a), 4(a), and 5(a) for the deviation of magnetic parameter (M), viscosity parameter (R), and porosity parameter (m) of the HTBTP-SNFs model whereas the corresponding values of AE are plotted in subfigures 3(b), 4(b), and 5(b) in order to obtain the execution of the HTBTP-SNFs approach. The reliable overlapping of analytic and numerical solutions can be detected. The impact of magnetic turf (M) on $f'(\eta)$ is presented in subfigure 3(a), which shows that when the magnetic field increase the velocity decreases. This is due to the reality that the increasing M develops the friction force of the movement and is identified as the Lorentz force. In the boundary sheet, Lorentz force has the correspondence to reduce the flow velocity. The influence of porosity parameter m on $f'(\eta)$ has been exposed in subfigure 4(a). The graph shows that when the porosity increases and the magnetic field is kept constant, the velocity profile increase in interval 0 to 0.5 and decrease in interval 0.5 to 1. Similarly, the impact of viscosity parameter R on $f'(\eta)$ has displayed in subfigure 5(a). It is obvious that when viscosity parameter (R) escalates with constant porous medium and magnetic field, the velocity of the fluid escalates in interval 0 to 0.5 and decrease in interval 0.5 to 1.

Accordingly, the outcomes of temperature profile $\theta(\eta)$ are given in subfigures 6(a), 7(a), 8(a), and 9(a) of the HTBTP-SNFs model. The relevant values of AE are plotted in subfigures 6(b), 7(b), 8(b), and 9(b) for the HTBTP-SNFs model. It is observed from subfigure 6(a) that escalating Nb reduces the temperature field. Actually, escalating Nb kinetic

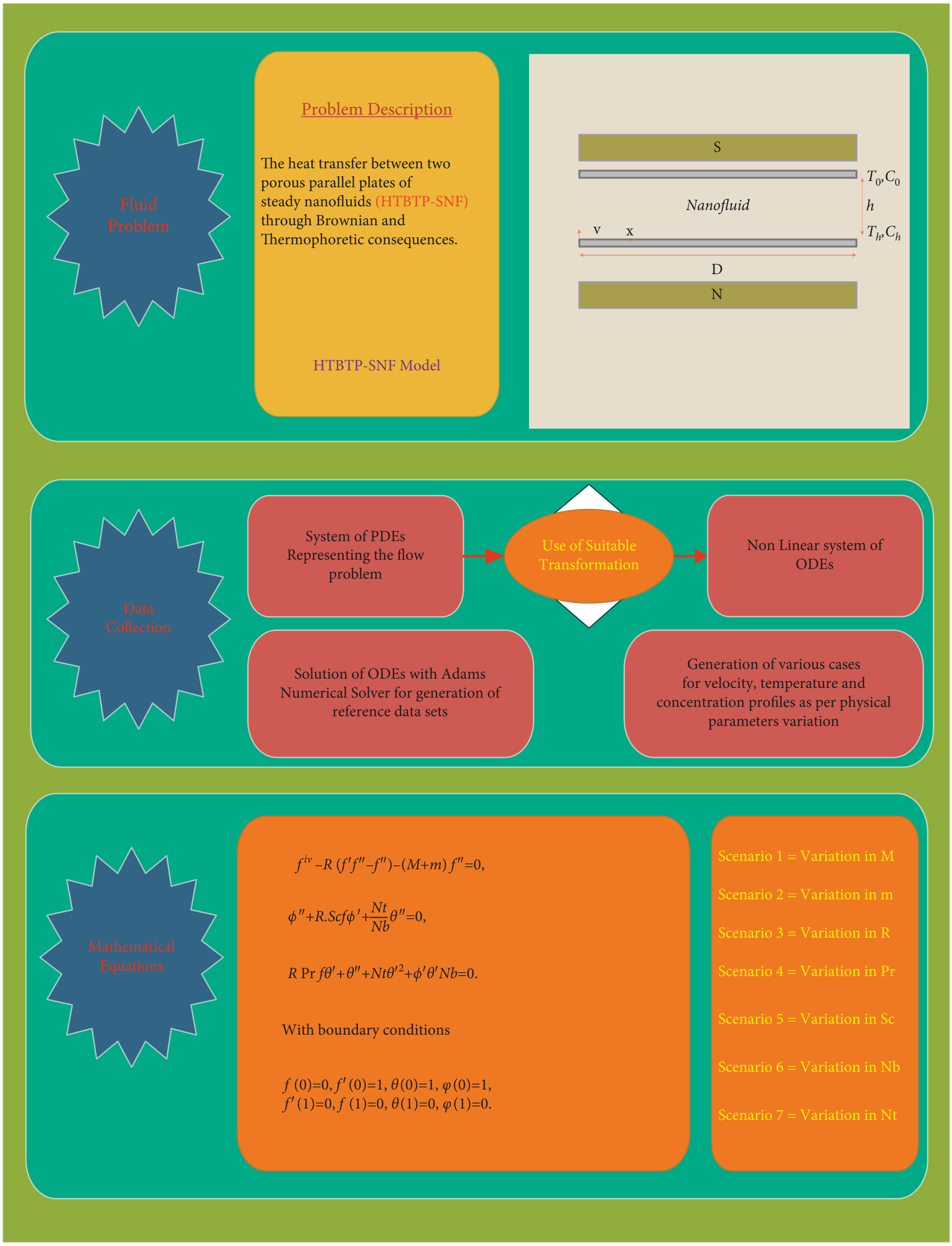

Figure 2: Overall working flowchart.

energy increases due to which the nanoparticles within the fluid raise the heat transfer rate and boundary thickness coating, which decrease the temperature field. Subfigure 7(a) shows the effect of the thermophoretic parameter on $\theta(\eta)$. It is clear from subfigure 7(a) that when value of Nt escalates, the temperature field is decreased. This is because of the reality that the thermophoresis parameter (Nt) depend on the gradient of temperature in the nearby nanofluid molecules. Escalating Nt decreases the kinetic energy of the nanofluid molecule, which results in the decrement in the temperature distribution. The influence of Pr on temperature distributions is presented in subfigure 8(a), temperature profile vary directly with Pr. The greater value of Pr causes decrement in the temperature profile. Subfigure 9(a) displays

Table 4: Scenarios interpretation beside with cases for the HTBTP-SNFs model.

Scenarios	Cases	Physical measures of concern						
		M	m	R	Pr	Sc	Nb	Nt
1	1	1	1	1	1	0.7	0.1	0.1
	2	2	1	1	1	0.7	0.1	0.1
	3	3	1	1	1	0.7	0.1	0.1
2	1	1	1	1	1	0.7	0.1	0.1
	2	1	3	1	1	0.7	0.1	0.1
	3	1	5	1	1	0.7	0.1	0.1
3	1	1	1	1	1	0.7	0.1	0.1
	2	1	1	3	1	0.7	0.1	0.1
	3	1	1	5	1	0.7	0.1	0.1
4	1	1	1	1	1	0.7	0.1	0.1
	2	1	1	1	2	0.7	0.1	0.1
	3	1	1	1	3	0.7	0.1	0.1
5	1	1	1	1	1	1	0.1	0.1
	2	1	1	1	1	2	0.1	0.1
	3	1	1	1	1	3	0.1	0.1
6	1	1	1	1	1	0.7	0.1	0.1
	2	1	1	1	1	0.7	0.2	0.1
	3	1	1	1	1	0.7	0.3	0.1
7	1	1	1	1	1	0.7	0.1	0.1
	2	1	1	1	1	0.7	0.1	0.2
	3	1	1	1	1	0.7	0.1	0.3

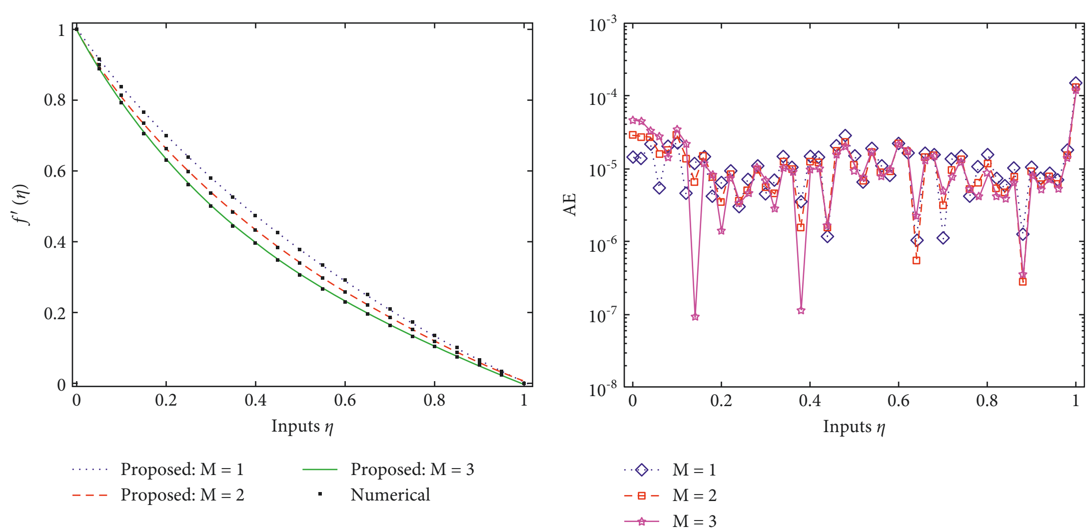

(a) (b)

Figure 3: (a) Influence of M. (b) Analysis on AE.

the impact of viscosity parameter (R) on temperature distribution, which shows the direct relation when R increases and the temperature distribution is deaccelerated. This decrement caused by the increase of inertial force, which increase with incensement in R. Because when the values of viscosity parameter (R) increase, the inertial forces get strong and the temperature field has a tendency to decrease. Furthermore, between numerical and analytical effects, these results also show the uniform overlapping.

Similarly, the outcomes of concentration distribution $\varphi(\eta)$ are given in subfigures 10(a), 11(a), and 12(a) of the HTBTP-SNFs model. The appropriate values of AE are mapped in subfigures 10(b), 11(b), and 12(b). Subfigure 10(a) indicates the effect of Schmidt quantity (Sc) on concentration profile $\varphi(\eta)$, where Sc represent momentum and mass diffusivity ratio. Subfigure 11(a) explains the influence of thermophoresis parameter (Nt) on $\varphi(\eta)$. It is clear from subfigure 11(a) that when value of Nt increase the concentration field decreases. Escalating Nt decreases the kinetic energy of the nanofluid molecule, which causes the decrement in the concentration profile. It is observed from subfigure 12(a) that increasing Nb reduces the concentration

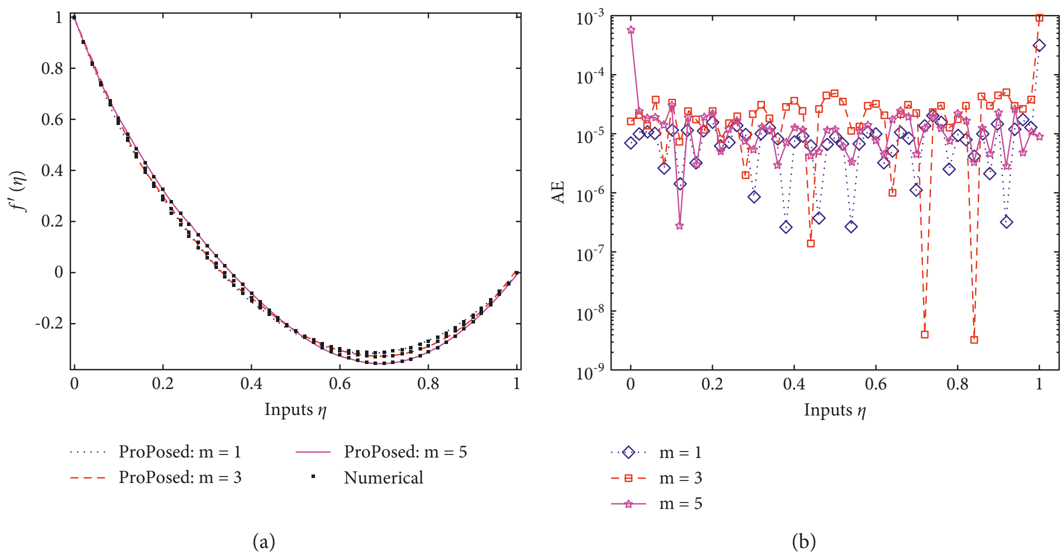

FIGURE 4: (a) Influence of m. (b) Analysis on AE.

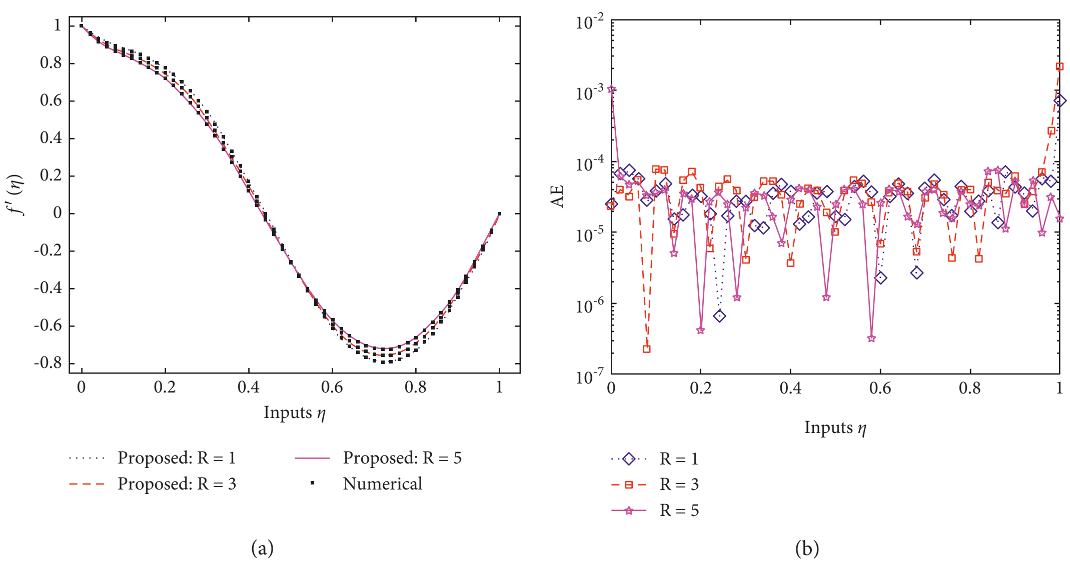

FIGURE 5: (a) Influence of R. (b) Analysis on AE.

field. The concentration profile reduces by increasing the Brownian motion parameter (Nb). The boundary coating thicknesses decreases because of rise of Brownian motion, which cause to reduce concentrations. These results also show the consistent overlapping between analytical and numerical solution.

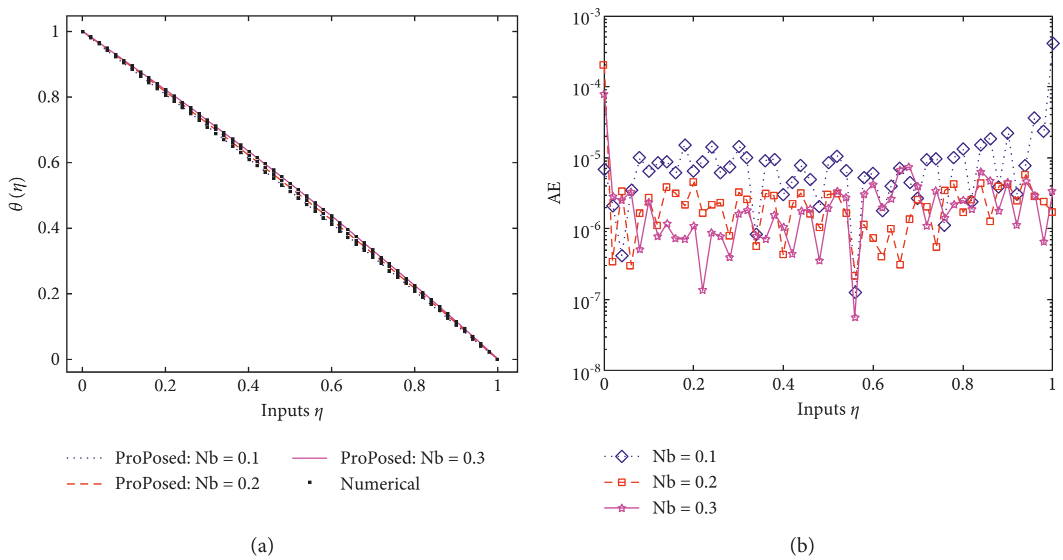

Figure 6: (a) Influence of Nb. (b) Analysis on AE.

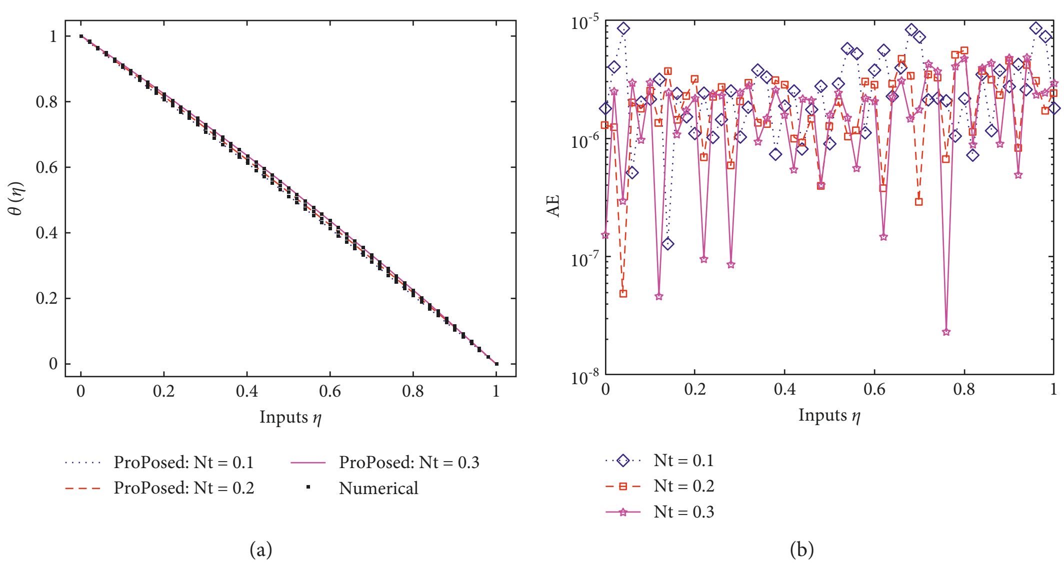

Figure 7: (a) Influence of Nt. (b) Analysis on AE.

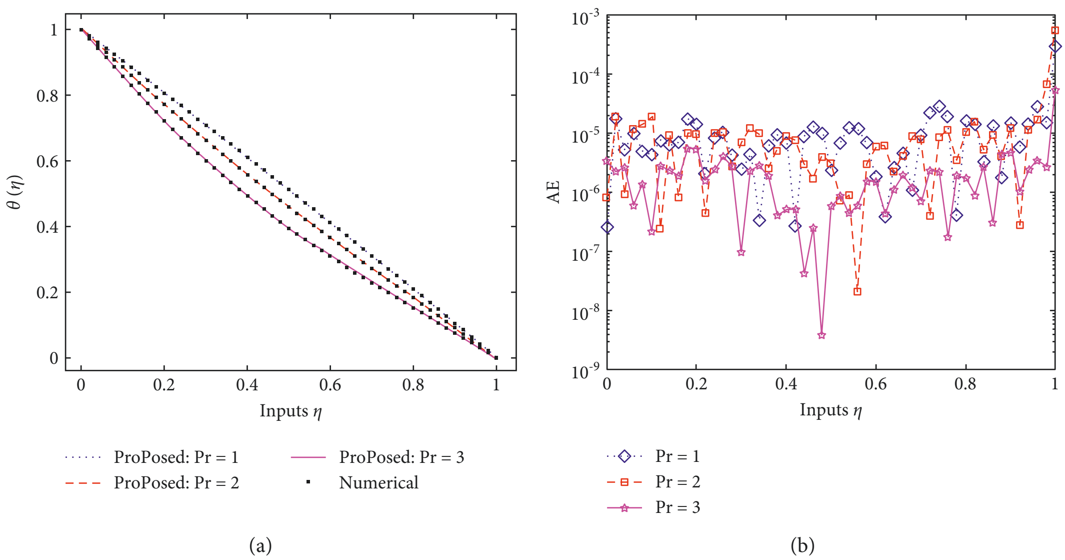

Figure 8: (a) Influence of Pr. (b) Analysis on AE.

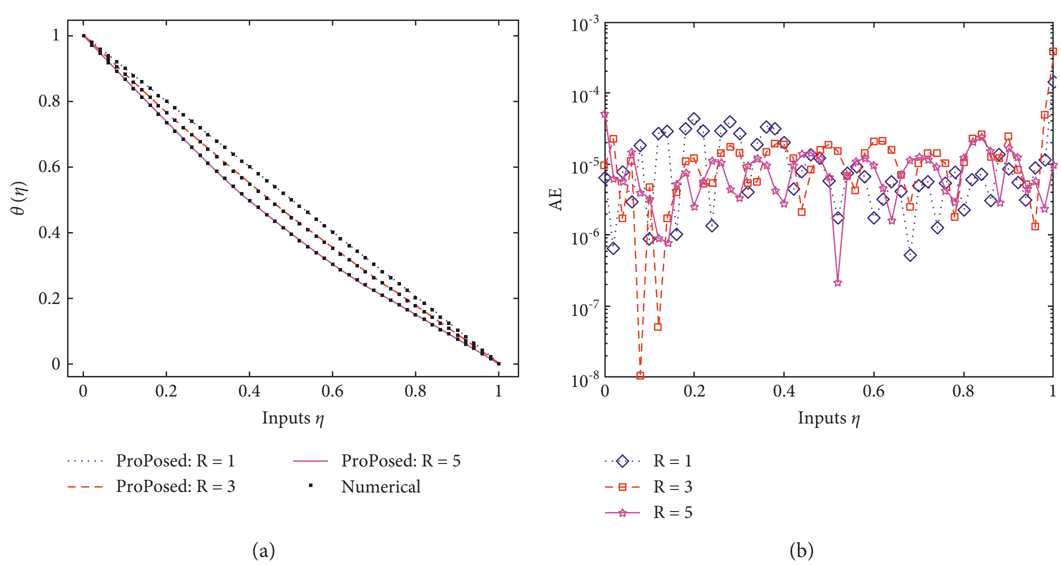

Figure 9: (a) Influence of R. (b) Analysis on AE.

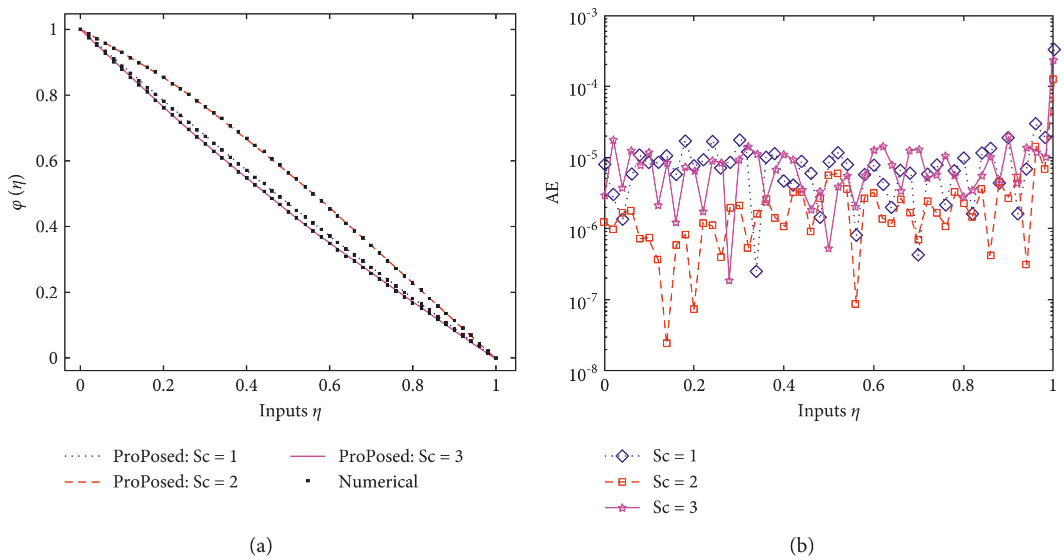

Figure 10: (a) Influence of Sc. (b) Analysis on AE.

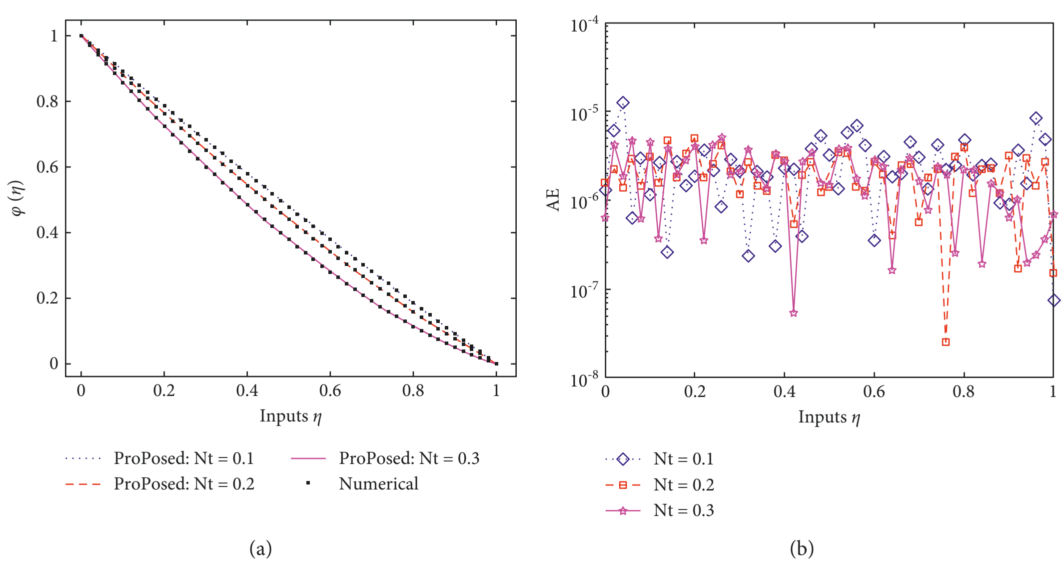

Figure 11: (a) Influence of Nt. (b) Analysis on AE.

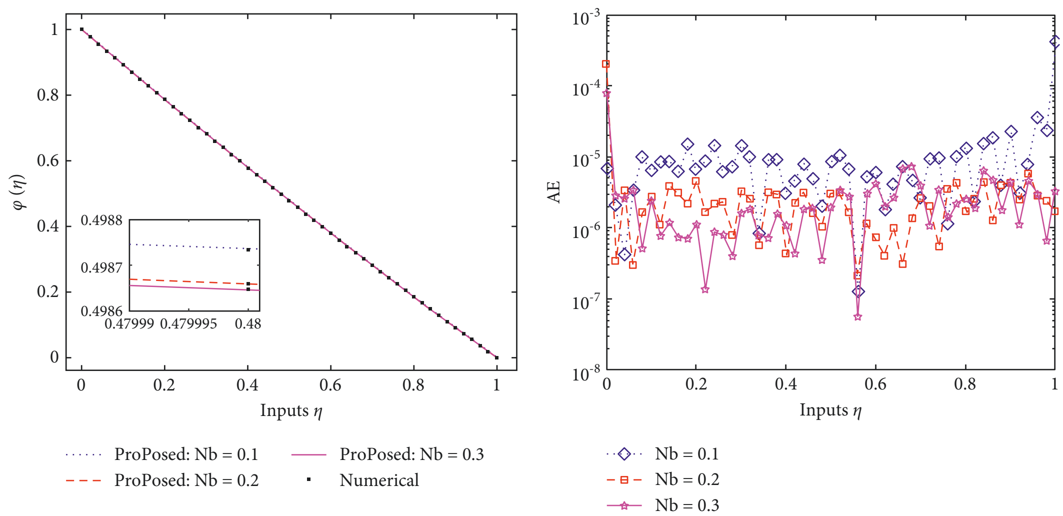

(a) (b)

FIGURE 12: (a) Influence of Nb. (b) Analysis on AE.

5. Comparison Tables of the OAFM and Adams Numerical Method

6. Conclusion

In this analysis, a novel analytical technique for solving the boundary layer flow model was proposed (HTBTP-SNFs). The governing equations of the HTBTP-SNFs model are explained in first-order series, and the first-order solution is reached with excellent accuracy. We associated the OAFM findings with the numerical results produced using the Adams numerical technique to ensure the perfection and strength of our method. The comparison shows that the recommended approach is perfect, and the decent agreement of our consequences with the numerical data demonstrates the method's validity. Though the nonlinear beginning/boundary value issue does not comprise the tiny parameter, OAFM is extremely straightforward to apply to large nonlinear primary and boundary value problems. In compared to other analytical methods, OAFM is relatively simple to use and produces excellent results for more complicated nonlinear initial/boundary value issues. Since the OAFM contains the control convergence constansts, which are also known as optimal constants, we can control the convergence of the method. When compared to other approaches, OAFM requires less computing labor, and even a low-spec machine may readily complete the task. There are currently no limitations to this approach, allowing us to apply this effective and quick convergent method to increasingly complicated models originating from real-world situations in the future. The Adams numerical technique is a reliable numerical method for obtaining precise results. The Adams numerical method is an iterative technique that requires the most space and time, whereas OAFM is a short method that converges quickly. For addressing any nonlinear system of equations, both the Adams numerical technique and OAFM are good approaches.

The aim of the present research work is to present a novel application of comparative analysis of the new scheme paradigm (HTBTP-SNFs) of the heat transfer between two permeable parallel plates of steady nanofluids through Brownian and thermophoretic consequences. This comparative analysis of the HTBTP-SNFs model is based on the newly established optimal approach, namely, optimal auxiliary function method (OAFM) and the Adams numerical technique to find the analytical and numerical solutions of the HTBTP-SNFs model. Both results give a close resemblance of their approaches which indicates that both techniques converge quickly and both are strongly accurate and efficient methods.

Nomenclature

u, v:	Components of velocity
x, y:	Coordinates system
p^*:	Modified pressure
μ:	Fluid dynamic viscosity
C:	Nanoparticles concentration
Ci:	Specific heat of nanofluid
Nb:	Parameter of Brownian motion
θ:	Dimensionless temperature
T:	Fluid temperature
R:	Viscosity parameter
$^{D}\ T$:	Coefficient of thermophoresis diffusion
Sc:	Schmidt number
OAFM:	Optimal auxilary function method
t:	Time for steady flow
ϕ:	Dimensionless concentration
C_f:	Skin friction coefficient
B0:	Uniform magnetic field
M:	Magnetic parameter
D_B:	Brownian diffusion coefficient
m:	Parameter of porosity
Pr:	Prandlt quantity
Nu:	Nusselt number

ρ: Fluid density
ρ: Efficient heat capacity of nanoparticle
σ: Electrical conductivity heat transfer between two porous parallel plates of steady nanofluids.

Data Availability

All the data are available in the manuscript.

Conflicts of Interest

The authors declare that they have no conflicts of interest.

References

[1] D. M. Forrester, J. Huang, V. J. Pinfield, and F. Luppé, "Experimental verification of nanofluid shear-wave reconversion in ultrasonic fields," *Nanoscale*, vol. 8, no. 10, pp. 5497–5506, 2016.

[2] W. Yu and S. U. S. Choi, "The role of interfacal layers in the enhanced thermal conductivity of nanofluids: a renovated Maxwell model," *Journal of Nanoparticle Research*, vol. 5, no. 1-2, pp. 167–171, 2003.

[3] S. U. S. Choi and J. A. Eastman, "Enhancing thermal conductivity of fluids with nanoparticles," *Materials Science*, vol. 231, pp. 99–105, 1995.

[4] S. U. Choi and J. A. Eastman, *Enhancing thermal Conductivity of Fluids with Nanoparticles (No. ANL/MSD/CP-84938; CONF-951135-29)*, Argonne National Lab (ANL), Argonne, IL, USA, 1995.

[5] N. Shehzad, A. Zeeshan, R. Ellahi, and K. Vafai, "Convective heat transfer of nanofluid in a wavy channel: buongiorno's mathematical model," *Journal of Molecular Liquids*, vol. 222, pp. 446–455, 2016.

[6] Y. Xuan and Q. Li, "Investigation on convective heat transfer and flow features of nanofluids," *Journal of Heat Transfer*, vol. 125, no. 1, pp. 151–155, 2003.

[7] A. A. Mahmoud and E. Shimaa, "MHD flow and heat transfer of a micropolar fluid over a stretching surface with heat generation (absorption) and slip velocity," *Journal of the Egyptian Mathematical Society*, vol. 20, no. 1, pp. 20–27, 2012.

[8] F. Awad, M. S. Ahamed, P. Sibanda, and M. Khumalo, "The effect of thermophoresis on unsteady oldroyd-B nanofluid flow over stretching surface," *PLoS One*, vol. 10, no. 8, Article ID e0135914.

[9] S. Nadeem and S. T. Hussain, "Analysis of MHD williamson nano fluid flow over a heated surface," *Journal of Applied Fluid Mechanics*, vol. 9, no. 2, pp. 729–739, 2016.

[10] B. Mahanthesh, B. J. Gireesha, and R. Subba, "Unsteady three-dimensional MHD flow of a nano Eyring-Powell fluid past a convectively heated stretching sheet in the presence of thermal radiation, viscous dissipation and Joule heating," *Journal of the Association of Arab Universities for Basic and Applied Sciences*, vol. 23, no. 1, pp. 75–84.

[11] M. Khan, R. Mali, A. Munir, and W. A. Khan, "Flow and heat transfer to Sisko nanofluid over a nonlinear stretching sheet," *PLoS One*, vol. 10.

[12] S. Qayyum, T. Hayat, A. Alsaedi, and B. Ahmad, "Magnetohydrodynamic (MHD) nonlinear convective flow of Jeffrey nanofluid over a nonlinear stretching surface with variable thickness and chemical reaction," *International Journal of Mechanical Sciences*, vol. 134, pp. 306–314, 2017.

[13] S. Witharana, H. Chen, and Y. Ding, "Stability of nanofluids in quiescent and shear flow fields," *Nanoscale Research Letters*, vol. 6, no. 1, p. 231, 2011.

[14] S. Zeinali Heris, S. G. Etemad, and M. Nasr Esfahany, "Experimental investigation of oxide nanofluids laminar flow convective heat transfer," *International Communications in Heat and Mass Transfer*, vol. 33, no. 4, pp. 529–535, 2006.

[15] R. Taylor, S. Coulombe, T. Otanicar et al., "Small particles, big impacts: a review of the diverse applications of nanofluids," *Journal of Applied Physics*, vol. 113, no. 1, pp. 1–8, 2013.

[16] J. Buongiorno, "Convective transport in nanofluids," *Journal of Heat Transfer*, vol. 128, no. 3, pp. 240–250, 2006.

[17] R. Y. Jou and S. C. Tzeng, "Numerical research of nature convective heat transfer enhancement filled with nanofluids in rectangular enclosures," *International Communications in Heat and Mass Transfer*, vol. 33, no. 6, pp. 727–736, 2006.

[18] M. M. Rashidi, S. Abelman, S. Abelman, and N. Freidooni Mehr, "Entropy generation in steady MHD flow due to a rotating porous disk in a nanofluid," *International Journal of Heat and Mass Transfer*, vol. 62, pp. 515–525, 2013.

[19] F. Garoosi, G. Bagheri, and M. M. Rashidi, "Two phase simulation of natural convection and mixed convection of the nanofluid in a square cavity," *Powder Technology*, vol. 275, pp. 239–256, 2015.

[20] F. Garoosi, B. Rohani, and M. M. Rashidi, "Two-phase mixture modeling of mixed convection of nanofluids in a square cavity with internal and external heating," *Powder Technology*, vol. 275, pp. 304–321, 2015.

[21] F. Garoosi, L. Jahanshaloo, M. M. Rashidi, A. Badakhsh, and M. E. Ali, "Numerical simulation of natural convection of the nanofluid in a heat exchangers using a Buongiorno model," *Applied Mathematics and Computation*, vol. 254, pp. 183–203, 2015.

[22] H. R. Ashorynejad, M. Sheikholeslami, I. Pop, and D. D. Ganji, "Nanofluid flow and heat transfer due to a stretching cylinder in the presence of magnetic field," *Heat and Mass Transfer*, vol. 49, no. 3, pp. 427–436, 2013.

[23] H. R. Ashorynejad, A. A. Mohamad, M. Sheikholeslami, I. Pop, and D. D. Ganji, "Magnetic field effects on natural convection flow of a nanofluid in a horizontal cylindrical annulus using Lattice Boltzmann method," *International Journal of Thermal Sciences*, vol. 64, pp. 240–250, 2013.

[24] M. Hatami, M. Sheikholeslami, M. Hosseini, and D. D. Ganji, "Analytical investigation of MHD nanofluid flow in non-parallel walls," *Journal of Molecular Liquids*, vol. 194, pp. 251–259, 2014.

[25] M. Hatami, M. Sheikholeslami, and D. D. Ganji, "Nanofluid flow and heat transfer in an asymmetric porous channel with expanding or contracting wall," *Journal of Molecular Liquids*, vol. 195, pp. 230–239, 2014.

[26] M. Hatami, M. Sheikholeslami, D. D. Ganji, and D. D. Ganji, "RETRACTED: laminar flow and heat transfer of nanofluid between contracting and rotating disks by least square method," *Powder Technology*, vol. 253, pp. 769–779, 2014.

[27] D. Domairry, M. Sheikholeslami, H. R. Ashorynejad, R. S. R. Gorla, and M. Khani, "Natural convection flow of a non-Newtonian nanofluid between two vertical flat plates," *Proceedings of the Institution of Mechanical Engineers - Part N: Journal of Nanoengineering and Nanosystems*, vol. 225, no. 3, pp. 115–122, 2012.

[28] H. Chen, S. Witharana, Y. Jin, C. Kim, and Y. Ding, "Predicting thermal conductivity of liquid suspensions of nanoparticles (nanofluids) based on rheology," *Particuology*, vol. 7, no. 2, pp. 151–157, 2009.

[29] S. K. Das, U. C. H. Stephen, Y. Wenhua, and T. Pradeep, *Nanofluids: Science and Technology*, Wiley-Interscience, Hoboken, NJ, USA, 2010.

[30] A. Zubaidi, M. Nazeer, S. Saleem, F. Hussain, and F. Ahmad, "Flow of nanofluid towards a Riga surface with heat and mass transfer under the effects of activation energy and thermal radiation," *International Journal of Modern Physics B*, vol. 35, no. 26, Article ID 2150266, 2021.

[31] H. Chen, S. Saleem, and M. Ghaderi, "Using artificial neural network to optimize the flow and natural heat transfer of a magnetic nanofluid in a square enclosure with a fin on its vertical wall: a Lattice Boltzmann simulation," *Journal of Thermal Analysis and Calorimetry*, vol. 145, 2021.

[32] R.-Y. Jou and S.-C. Tzeng, "Numerical research of nature convective heat transfer enhancement filled with nanofluids in rectangular enclosures," *International Communications in Heat and Mass Transfer*, vol. 33, no. 6, pp. 727–736, 2006.

[33] M. M. Rashidi and S. A. M. Pour, "Analytic approximate solutions for steady flow over a rotating disk in porous medium by homotopy analysis method with two auxiliary parameters," *International Journal of Applied Mathematics & Statistics*, 2010.

[34] M. M. Rashidi, S. Abelman, and N. Freidooni Mehr, "Entropy generation in steady MHD flow due to a rotating porous disk in a nanofluid," *International Journal of Heat and Mass Transfer*, vol. 62, pp. 515–525, 2013.

[35] M. Veera Krishna, "Heat transport on steady MHD flow of copper and alumina nanofluids past a stretching porous surface," *Heat Transfer*, vol. 49, no. 3, pp. 1374–1385, 2020.

[36] P. Lin and A. Ghaffari, "Heat and mass transfer in a steady flow of Sutterby nanofluid over the surface of a stretching wedge," *Physica Scripta*, vol. 96, no. 6, Article ID 065003, 2021.

[37] C. Fetecau, D. Vieru, and A. Zeeshan, "Analytical solutions for two mixed initial-boundary value problems corresponding to unsteady motions of Maxwell fluids through a porous plate channel," *Mathematical Problems in Engineering*, vol. 2021, Article ID 5539007, 13 pages, 2021.

[38] A. Zeeshan, A. Riaz, and F. Alzahrani, "Electroosmosis-modulated bio-flow of nanofluid through a rectangular peristaltic pump induced by complex traveling wave with zeta potential and heat source," *Electrophoresis*, vol. 42, no. 21-22, pp. 2143–2153, 2021.

[39] M. S. Abel, M. M. Nandeppanavar, and S. B. Malipatil, "Heat transfer in a second grade fluid through a porous medium from a permeable stretching sheet with non-uniform heat source/sink," *International Journal of Heat and Mass Transfer*, vol. 53, no. 9-10, pp. 1788–1795, 2010.

[40] M. M. Rashidi, E. Momoniat, and B. Rostami, "Analytic approximate solutions for MHD boundary-layer viscoelastic fluid flow over continuously moving stretching surface by homotopy analysis method with two auxiliary parameters," *Journal of Applied Mathematics*, vol. 2012, Article ID 780415, 19 pages, 2012.

[41] S. Khalili, H. Tamim, A. Khalili, and M. M. Rashidi, "Unsteady convective heat and mass transfer in pseudoplastic nanofluid over a stretching wall," *Advanced Powder Technology*, vol. 26, no. 5, pp. 1319–1326, 2015.

[42] M. H. Abolbashari, N. Freidoonimehr, F. Nazari, and M. M. Rashidi, "Analytical modeling of entropy generation for Casson nano-fluid flow induced by a stretching surface," *Advanced Powder Technology*, vol. 26, no. 2, pp. 542–552, 2015.

[43] M. M. Rashidi, T. Hayat, M. Keimanesh, and H. Yousefian, "A study on heat transfer in a second-Grade fluid through a porous medium with the modified differential transform method," *Heat Transfer - Asian Research*, vol. 42, 2013.

[44] M. Irani, M. Afrand, and B. Mehmandoust, "Curve fitting on experimental data of a new hybrid nano-antifreeze viscosity: presenting new correlations for non- Newtonian nanofluid," *Physica A: Statistical Mechanics and Its Applications*, vol. 531, Article ID 120837, 2019.

[45] P. M. Nafchi, A. Karimipour, and M. Afrand, "The evaluation on a new non-Newtonian hybrid mixture composed of TiO2/ZnO/EG to present a statistical approach of power law for its rheological and thermal properties," *Physica A: Statistical Mechanics and Its Applications*, vol. 516, pp. 1–18, 2019.

[46] C. Amanulla, A. Wakif, Z. Boulahia, S. Fazuruddin, and S. Noor Mohammed, "A study on non-Newtonian transport phenomena in MHD fluid flow from a vertical cone with Navier slip and convective heating," *Nonlinear Engineering*, vol. 8, no. 1, pp. 534–545, 2019.

[47] I. Kazemi, M. Sefid, and M. Afrand, "A novel comparative experimental study on rheological behavior of mono & hybrid nanofluids concerned graphene and silica nano-powders: c," *Powder Technology*, vol. 366, pp. 216–229, 2020.

[48] M. S. Iqbal, I. Mustafa, A. Ghaffari, and Usman, "A computational analysis of dissipation effects on the hydromagnetic convective flow of hybrid nanofluids along a vertical wavy surface," *Heat Transfer*, vol. 50, no. 8, pp. 8035–8051, 2021.

[49] A. Ghaffari, I. Mustafa, T. Muhammad, and Y. Altaf, "Analysis of entropy generation in a power-law nanofluid flow over a stretchable rotatory porous disk," *Case Studies in Thermal Engineering*, vol. 28, Article ID 101370, 2021.

[50] H. Yaghoobi and M. Torabi, "The application of differential transformation method to nonlinear equations arising in heat transfer," *International Communications in Heat and Mass Transfer*, vol. 38, no. 6, pp. 815–820, 2011.

[51] J. H. He, "Homotopy perturbation technique," *Computer Methods in Applied Mechanics and Engineering*, vol. 178, pp. 257–262, 1999.

[52] D. D. Ganji, "The application of He's homotopy perturbation method to nonlinear equations arising in heat transfer," *Physics Letters A*, vol. 355, no. 4-5, pp. 337–341, 2006.

[53] R. Bellman, *Perturbation Techniques in Mathematics, physics, and engineering*, New York, Holt, Rinehart and Winston, New York, NY, USA, 1964.

[54] S. H. Chowdhury, "A comparison between the modified homotopy perturbation method and adomian decomposition method for solving nonlinear heat transfer equations," *Journal of Applied Sciences*, vol. 11, no. 8, pp. 1416–1420, 2011.

[55] D. D. Ganji, G. A. Afrouzi, and R. A. Talarposhti, "Application of variational iteration method and homotopy-perturbation method for nonlinear heat diffusion and heat transfer equations," *Physics Letters A*, vol. 368, no. 6, pp. 450–457, 2007.

[56] H. Yaghoobi and M. Torabi, "The application of differential transformation method to nonlinear equations arising in heat

transfer," *International Communications in Heat and Mass Transfer*, vol. 38, no. 6, pp. 815–820, 2011.

[57] S. J. Liao, *The proposed homotopy analysis technique for the solution of nonlinear problems*, PhD Thesis, Shanghai Jiao Tong University, Shanghai, China, 1992.

[58] G. L. Liu, "New research direction in singular perturbation theory: artificial parameter approach and inverse perturbation technique," in *Proceedings of the 7th Conference on Modern Mathematics and Mechanics*, Shanghai, China, September 1997.

[59] N. Herisanu and V. Marinca, "An efficient analytical approach to investigate the dynamics of a misaligned multirotor system," *Mathematics*, vol. 8, no. 7, p. 1083, 2020.

[60] N. Herisanu, V. Marinca, G. Madescu, and F. Dragan, "Dynamic response of a permanent magnet synchronous generator to a wind gust," *Energies*, vol. 12, no. 5, p. 915, 2019.